PROCEEDINGS OF SCIENCE

First measurement of heavy flavour femtoscopy using D^0 mesons and charged hadrons in Au+Au collisions at $\sqrt{s_{NN}}$ = 200 GeV by STAR

Priyanka Roy Chowdhury[a] **and Katarzyna Gwiździel**[a,*] **on behalf of the STAR Collaboration**

[a] *Faculty of Physics, Warsaw University of Technology, Koszykowa 75, Warsaw, Poland*
E-mail: priyanka.roy_chowdhury.dokt@pw.edu.pl, katarzyna.gwizdziel.dokt@pw.edu.pl

Heavy quarks are produced in hard partonic scatterings at the very early stage of heavy-ion collisions and experience the whole evolution of the Quark-Gluon Plasma medium. Two-particle femtoscopic correlations at low relative momentum are sensitive to the final-state interactions and to the space-time extent of the region from which the correlated particles are emitted. Correlations study between the charmed mesons and identified charged hadrons can shed light on their interactions in the hadronic phase and the interaction of charm quarks with the medium.

We will report the measurement of femtoscopic correlations between D^0 and charged hadrons at mid-rapidity in Au+Au collisions at $\sqrt{s_{NN}}$ = 200 GeV by the STAR experiment. D^0 mesons are reconstructed via the $K^-\pi^+$ decay channel using topological criteria enabled by the Heavy Flavor Tracker. We will compare the experimental data with available theoretical models to discuss their physics implications.

42nd International Conference on High Energy Physics (ICHEP2024)
18-24 July 2024
Prague, Czech Republic

*Speaker

1. Introduction

Experiments at the Relativistic Heavy Ion Collider (RHIC) and the Large Hadron Collider (LHC) allow us to study various physical phenomena. One of the objects of interest is the so-called Quark-Gluon Plasma (QGP). This state of matter is created in high-energy heavy-ion collisions and is described by quark and gluonic degrees of freedom. The properties of QGP can be examined using heavy quarks, like charm ($c/\overline{c}$) and bottom ($b/\overline{b}$) quarks. Due to their large mass, they are produced very early in the reaction (before the QGP phase). Therefore, they are valuable probes for exploring all stages of heavy-ion collision: the QGP formation, the hadronization process, the chemical freeze-out, and more. Research dedicated to the QGP will help us better understand what happened after the Big Bang as well as the space-time evolution of the Universe [1, 2].

One of the main aims of the STAR experiment at RHIC is to study the QGP properties [3–5]. To do so, one can perform measurements with, for instance, charmed mesons like D^0 and $\overline{D^0}$ (mean lifetime $c\tau = 123.01$ μm [6]), which consist of one charm ($c/\overline{c}$) and one light quark ($u/\overline{u}$). So far, for D^0 mesons STAR reported a suppression for high-p_T region [7] and significant elliptic flow [8]. It suggests that charm quarks strongly interact with the medium and exhibit collective behaviour. Several theoretical calculations with various assumptions can reproduce the data.

Our knowledge about charm-medium interaction can be improved by measuring new observables, such as the two-particle momentum correlation function. It can help to constrain various theoretical models' parameters.

2. Methodology

Femtoscopy is a technique which allows us to study the space-time geometry of the matter produced in high-energy heavy-ion collisions using particle correlations in momentum space. According to the Koonin-Pratt formula [9], the correlation function $C(k^*)$ can be described as follows:

$$C(k^*) = \int S(r^*)|\Psi(\vec{r^*}, \vec{k^*})|^2 d^3r^*, \tag{1}$$

where k^* is a reduced momentum difference ($k^* = |\vec{k^*}| = \frac{1}{2}|\vec{p_2^*} - \vec{p_1^*}|$) and r^* is a relative separation vector ($r^* = |\vec{r^*}|$). The so-called source function $S(r^*)$ and pair wave function $\Psi(\vec{r^*}, \vec{k^*})$ contains the distribution of the relative distance in the pair rest frame and interaction, respectively. The correlation function is sensitive to the Final State Interactions (FSI, Coulomb and Strong) and Quantum Statistics (QS, Bose-Einstein and Femri-Dirac) [9]. In the case of $D^0/\overline{D^0}$-$h^\pm$ femtoscopic correlations, only strong interaction contributes to the correlation function. The $D^0/\overline{D^0}$ mesons are neutral particles, so there is no Coulomb interaction as well as the QS because the analyzed particle pairs are non-identical.

The correlation function provides the size and form of the phase space cloud of outgoing particle pairs. This region is a so-called area of homogeneity, and it is sensitive to the dynamics of QGP, for instance, to collective flow. If the correlations are strong, then the area of homogeneity dimension is significantly smaller than the size of the total source volume [10]. The radius (r) of the emission source can be determined using the $D^0/\overline{D^0}$-$h^\pm$ correlation functions.

3. Experimental setup and dataset

The STAR detector consists of several subsystems constructed to study thousands of particles produced by each nuclear collision [11]. The main subsystems for this analysis are the Time Projection Chamber (TPC), the Time of Flight (TOF) detector and the Heavy Flavour Tracker (HFT). The first two detectors (TPC and TOF) are used to track and identify charged particles. In this study, they are utilized for charged hadron identification (primary $K^{\pm}$, $\pi^{\pm}$, $p^{\pm}$). In 2013, the HFT [12] was installed in the STAR detector and included in data-taking campaigns in 2014 and 2016. It is a silicon detector designed to track open heavy-flavour hadrons. In this study, it is a crucial system used for the topological reconstruction of the secondary decay vertex of $D^0(\overline{D^0})$ meson.

The dataset used in this analysis consists of Au+Au collisions at $\sqrt{s_{NN}}$ = 200 GeV registered by the STAR experiment in the 2014 year run. The analyzed sample has around 600 M good minimum bias events.

4. Event and particle selection

In order to ensure good quality of the event selection with 0-80% centrality, the following criteria were applied: $|V_z| < 6$ cm, $|V_{xy}| < 2$ cm and $|V_z - V_z^{VPD}| < 3$ cm, where V_z and V_{xy} are the primary vertex positions of the collision alongside the z-axis and in the transverse plane, respectively, and V_z^{VPD} is the vertex position along the z-axis calculated using Vertex Position Detectors (VPDs, located on the both sides of the STAR detector). Thus, the collision point is determined based on the difference in the time of the signal registration in the left and right VPDs.

Information about ionization energy losses (dE/dx) from TPC and time-of-flight from TOF was used for track selection and identification. All tracks ($K^{\pm}$, $\pi^{\pm}$, $p^{\pm}$) were required to have the pseudorapidity from the range of $|\eta| < 1$ and at least 20 TPC hit points out of maximum 45 to ensure good momentum resolution. Then, the cuts for the resolution-normalized dE/dx deviation ($n\sigma$) from the expected value for each particle were applied [7]). For kaons, pions and protons, the cuts were as follows: $|n\sigma_K| < 3$, $|n\sigma_\pi| < 2$ and $|n\sigma_p| < 2$. Based on the information from the TOF detector, the cuts on the $|\Delta\frac{1}{\beta}|$ were applied, where Δ means deviation from the expected value and β is a particle velocity. The following cut was used for all tracks ($h^{\pm}$): $|\Delta\frac{1}{\beta}| < 0.03$. For $K^{\pm}$ and $\pi^{\pm}$ mesons, we required the momentum (p) to be less than 1 GeV/c and for protons $p < 1.2$ GeV/c.

5. D^0 reconstruction and purity estimation

$D^0(\overline{D^0})$ mesons were reconstructed through their hadronic decay channel into $K^-\pi^+$ ($K^+\pi^-$) pair. It was done with a branching ratio of 3.89% using topological criteria enabled by the HFT detector with outstanding track-pointing resolution. Figure 1 shows the invariant mass distributions of the reconstructed $D^0/\overline{D^0}$ candidates within a mass range of 1.73-2.00 GeV/c^2 for the background fit and 1.82-1.91 GeV/c^2 for the signal fit. Signal (S) over the combinatorial background (B) under the $D^0/\overline{D^0}$ peak increases with increasing transverse momentum (p_T). The $D^0/\overline{D^0}$ candidates with p_T from 1 to 10 GeV/c, rapidity $|y| < 1$, and good S/B ratio were selected for this study. For each p_T bin (1-2, 2-3, 3-5, 5-10 GeV/c), the D^0 signal purity [where purity = S/(S+B)] was calculated.

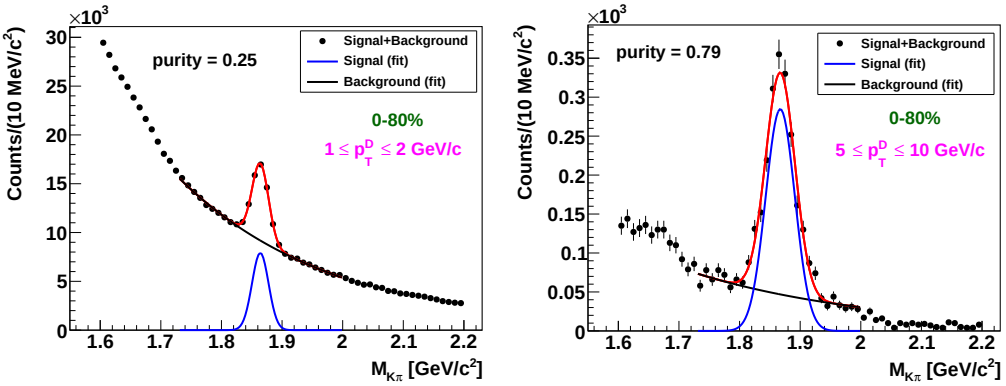

Figure 1: Invariant mass ($M_{K\pi}$) distributions of D^0 and $\overline{D^0}$ candidates for different $p_T$ranges from 0-80% centrality events. Solid black circles represent $D^0/\overline{D^0}$ signal [same event (SE), unlike-sign (US)] mixed with combinatorial background [SE, like sign (LS)]. Red and black lines are a Gaussian fit and an exponential fit to the background, respectively. The blue line shows the $D^0/\overline{D^0}$ signal fit with subtraction of SE, LS distributions within the mass range from 1.73 to 2.00 GeV/c^2.

6. Extraction of the correlation function

The correlation function for experimental data is calculated as the ratio of k^* distribution for correlated $[A(k^*)]$ to uncorrelated $[B(k^*)]$ particle pairs in the rest frame of their centre of mass and can be described as follows:

$$C(k^*) = N \cdot \frac{A(k^*)}{B(k^*)}, \tag{2}$$

where N is a normalization factor. The correlated pairs are particles coming from the same event. For uncorrelated pairs, the event mixing procedure is applied to extract the $B(k^*)$ distribution for tracks originating from different events but with similar z-vertex position (V_z) and centrality range.

The correlation function can be potentially affected by various unwanted effects. First, we alleviated the effects of the TPC detector, so we eliminated self-correlations between $D^0/\overline{D^0}$ mesons' daughters as well as track splitting (one track is treated as two separated tracks). These effects could have an impact on the number of correlated pairs. The next possible detector effect is track merging (two tracks are handled as one). The analysis disclosed minimal input from merged tracks. Besides the mentioned effects, we had to remove the contribution from the combinatorial background and the contamination of each identified hadron sample with other hadrons. To do so, the pair-purity correction was applied by implementing the following formula [13]:

$$C_{corr}(k^*) = \frac{C_{measured}(k^*) - 1}{PairPurity} + 1, \tag{3}$$

where $C_{corr}(k^*)$ and $C_{measured}(k^*)$ are, respectively, the final purity-corrected correlation function and the measured correlation function after corrections due to detector effects. The PairPurity is the product of the $D^0/\overline{D^0}$ meson signal purity and the average purity of the hadron ($K^{\pm}, \pi^{\pm}, p^{\pm}$) sample. The purity for each hadron was calculated within nσ fit in momentum bins using a sum of three Gaussian functions for kaons, pions and protons. The average purity for D^0 meson sample is around 37%, for K meson ~(97 ± 3 (syst.))%, for π meson ~(99.5 ± 0.5 (syst.))%, and for protons

~(99.5 ± 0.5 (syst.))%. Systematic uncertainties were calculated by varying the topological cuts for D^0 reconstruction, and they included the uncertainty on purity estimation for each D^0-$h^{\pm}$ pair. The final systematic uncertainty is determined to be less than 8%.

7. Results and summary

Figure 2 shows the femtoscopic correlation functions for all possible combinations of $D^0/\overline{D^0}$-$\pi^{\pm}$ pairs (left panel), $D^0/\overline{D^0}$-$p^{\pm}$ pairs (middle panel) and $D^0/\overline{D^0}$-$K^{\pm}$ pairs (right panel). All correlation functions are after pair-purity correction. In each case, the $C(k^*)$ distribution is around unity. It indicates no significant correlation for the studied pairs, and large fluctuations come up due to low statistics. Based on the correlation strength, we can draw a conclusion about the source size. We presume a large emission source size from the presented results due to either weak or no correlation.

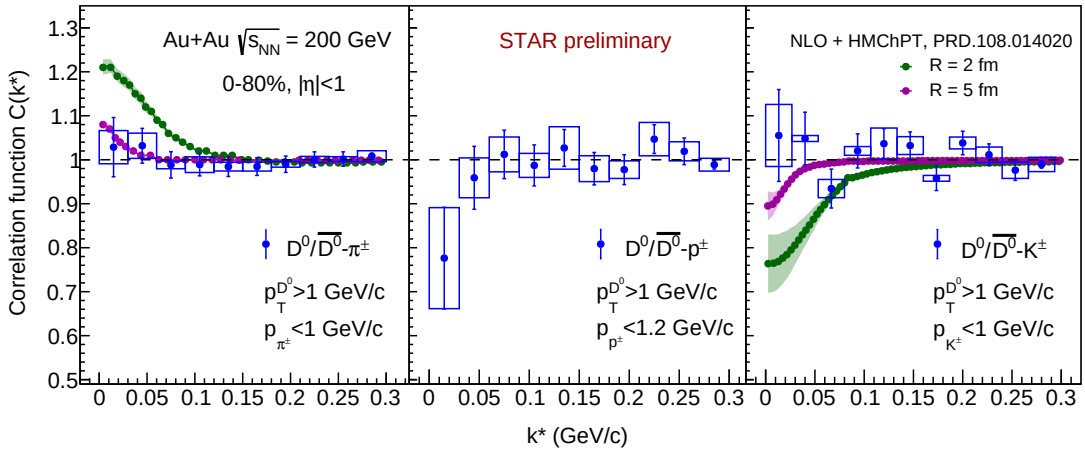

Figure 2: Femtoscopic correlation functions between $D^0/\overline{D^0}$ mesons and $\pi^{\pm}$ (left panel), $p^{\pm}$ (middle panel) and $K^{\pm}$ (right panel) pairs obtained for Au+Au collisions at $\sqrt{s_{NN}}$ = 200 GeV with $|\eta| < 1$. Blue solid points represent experimental data. They are shown with statistical and systematic (marked with boxes) uncertainties. In the case of $D^0/\overline{D^0}$-$\pi^{\pm}$and $D^0/\overline{D^0}$-$K^{\pm}$, the experimental data are compared with theoretical model predictions from [14] for source size of 2 fm (green band) and 5 fm (pink band).

We benchmarked the STAR data against available theoretical predictions obtained using the next-to-leading (NLO) order Heavy Meson Chiral Perturbation Theory (HMChPT) scheme [14]. We compared our correlation function for DK and Dπ pairs with the theoretical one calculted for the mixture of D^0K^+/D^+K^0 and $D^0\pi^+/D^+\pi^0$ pairs, respectively. In both cases, there is no Coulomb interaction. The STAR results for DK and Dπ pairs are consistent with the theoretical model predictions with an emission source size of 5 fm or larger. In the theoretical correlation function, the depletion, which increases with the decreasing source radius, can be observed. It is due to the existence of the $D^*_{S0}(2317)^{\pm}$ bound state. The effect is not visible in the STAR data. This is probably due to either a large emission source size or large experimental uncertainties.

The correlation function obtained for Dp pairs suggests a large emission source size, but theoretical predictions are necessary to conclude more about the results.

The presented results were obtained using the Run 2014 data. We expect that the observed femtoscopic correlations between $D^0/\overline{D^0}$ mesons and charged hadrons will be improved by using combined data from data-taking campaigns in 2014 and 2016. It will increase the precision of the reported measurement and will provide more decisive conclusions about the source size. Theoretical predictions are required for a better understanding of the data.

8. Acknowledgements

Priyanka Roy Chowdhury acknowledges financial support from National Science Centre, Poland (NCN) grant no. 2018/30/E/ST2/0008 and partial support by U.S Department of Energy (DOE).

References

[1] J. Rafelski, Eur. Phys. J. A **51** (2015) no.9, 114 doi:10.1140/epja/i2015-15114-0 [arXiv:1508.03260 [nucl-th]].

[2] X. Dong, Y. J. Lee and R. Rapp, Ann. Rev. Nucl. Part. Sci. **69** (2019), 417-445 doi:10.1146/annurev-nucl-101918-023806 [arXiv:1903.07709 [nucl-ex]].

[3] J. Adams *et al.* [STAR], Nucl. Phys. A **757** (2005), 102-183 doi:10.1016/j.nuclphysa.2005.03.085 [arXiv:nucl-ex/0501009 [nucl-ex]].

[4] M. I. Abdulhamid *et al.* [STAR], JHEP **06** (2023), 176 doi:10.1007/JHEP06(2023)176 [arXiv:2303.06590 [nucl-ex]].

[5] B. Aboona *et al.* [STAR], Phys. Rev. Lett. **130** (2023) no.11, 112301 doi:10.1103/PhysRevLett.130.112301 [arXiv:2207.06568 [nucl-ex]].

[6] R.L. Workman et al. (Particle Data Group), Prog.Theor.Exp.Phys. 2022, 083C01 (2022).

[7] J. Adam *et al.* [STAR], Phys. Rev. C **99** (2019) no.3, 034908 doi:10.1103/PhysRevC.99.034908 [arXiv:1812.10224 [nucl-ex]].

[8] L. Adamczyk *et al.* [STAR], Phys. Rev. Lett. **118** (2017) no.21, 212301 doi:10.1103/PhysRevLett.118.212301 [arXiv:1701.06060 [nucl-ex]].

[9] S. Acharya *et al.* [ALICE], Phys. Rev. D **110** (2024) no.3, 032004 doi:10.1103/PhysRevD.110.032004 [arXiv:2401.13541 [nucl-ex]].

[10] M. A. Lisa, S. Pratt, R. Soltz and U. Wiedemann, Ann. Rev. Nucl. Part. Sci. **55** (2005), 357-402 doi:10.1146/annurev.nucl.55.090704.151533 [arXiv:nucl-ex/0505014 [nucl-ex]].

[11] M. Harrison, T. Ludlam, and S. Ozaki, Nucl. Instr. Meth. Phys. Res. Sect. A **499**, No.2-3 (2003).

[12] H. Qiu (for the STAR Collaboration), Nuclear Physics A **931** (2014), 1141-1146, 0375-9474, https://doi.org/10.1016/j.nuclphysa.2014.08.056.

[13] J. Adams *et al.* [STAR], Phys. Rev. C **74** (2006), 064906 doi:10.1103/PhysRevC.74.064906 [arXiv:nucl-ex/0511003 [nucl-ex]].

[14] M. Albaladejo, J. Nieves and E. Ruiz Arriola, Phys. Rev. D **108** (2023), 014020 doi: https://doi.org/10.1103/PhysRevD.108.014020